Supporting information for

Greening Trends of Southern China Confirmed by GRACE

Le Chang and Wenke Sun *

Key Laboratory of Computational Geodynamics, University of Chinese Academy of Sciences, Beijing 100049, China; changle114@mails.ucas.ac.cn

* Correspondence:sunw@ucas.ac.cn; Tel.: +86-88256484

1. Introduction

Here, we introduce the geographical environment of Southern China in more detail. The soil water and groundwater datasets and processing method are also introduced in detail. We also provide the results of previous studies of the relationship between the leaf area index (LAI) and available soil water capacity.

2. The Significance Test of the Trend of GRACE.

The *p*-value is smaller than 0.05, which means that the trend is statistically significant with a 95% confidence interval. As shown in Figure S1, the *p*-values were calculated for the time series at each point detected by GRACE. We can see that the p-values within our study are very small, meaning that the trends are highly significant.

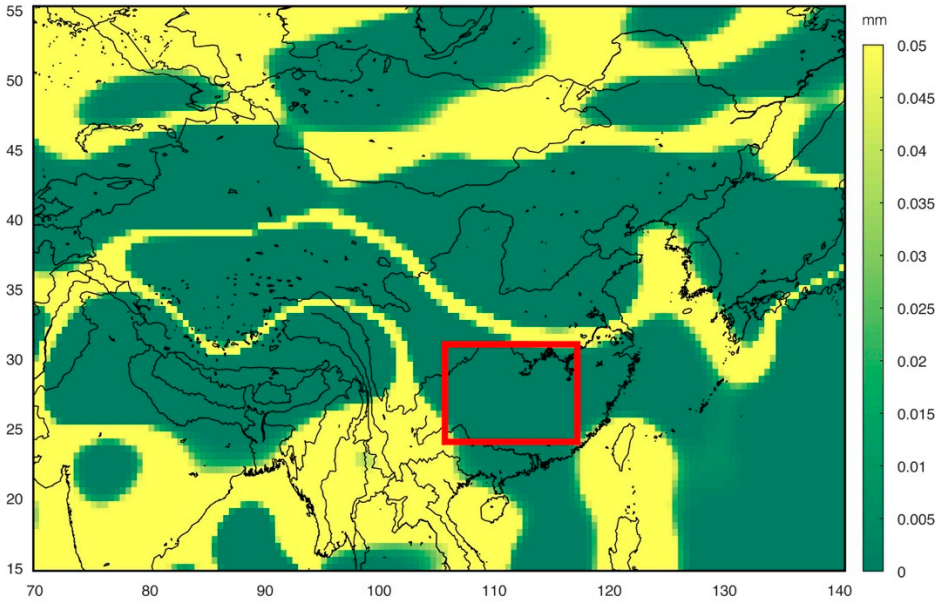

Figure S1. The distribution of *p*-values across our study region.

3. Large Lakes

There are two large lakes in our study region: Dongting Lake and Poyang Lake (see Figure S2a). The water level of these two lakes increased slightly in our study period. Yi et al. [2] studied the trend of each lake from 2003 to 2010, and the results are shown in Figures S2. We assume that their water levels increased 0.02 ± 0.08 m/yr from January 2003 to August 2016. We obtained the boundary of both lakes from digital elevation data. As a lake is not like the Three Gorges Reservoir, which exhibits large terrain changes, we also assumed that the boundaries did not change in our study period. We obtained the patterns of lake level

trends and converted them to spherical harmonic coefficients in up to degree 60 and smoothed them with the DDK4 filter. The signals of those two lakes are quite small, and we could not see obvious increasing signals as in the Three Gorges Reservoir, so we did not show the pattern of lake level change after smoothing and truncation.

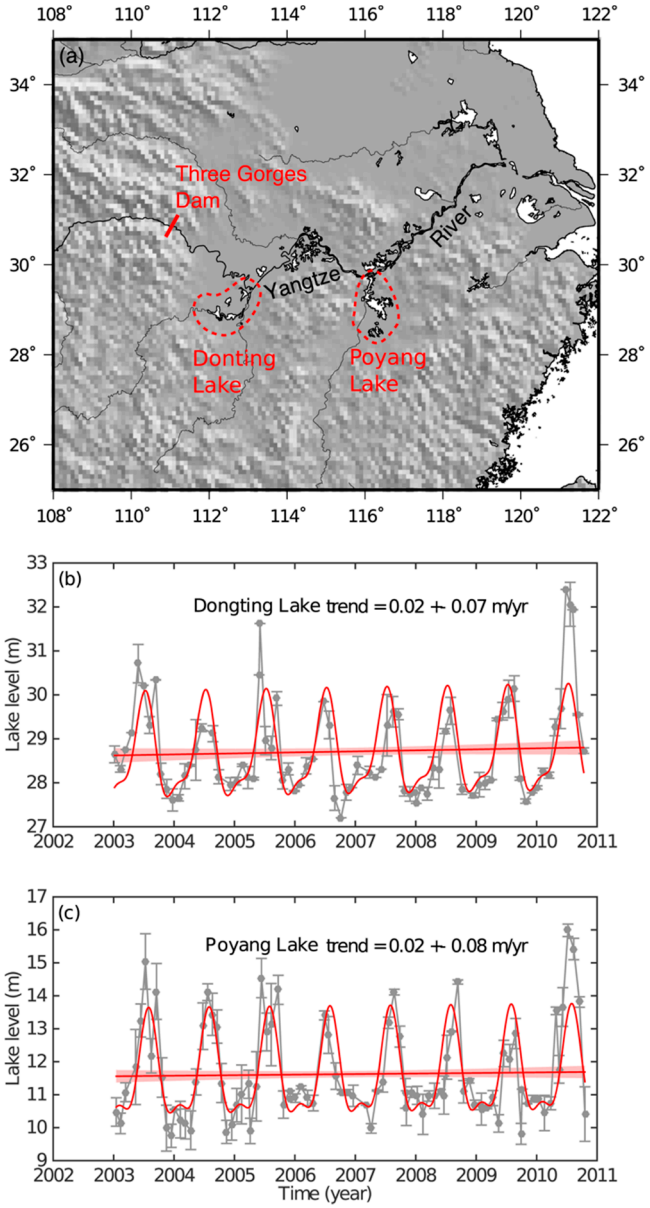

Figure S2. (a) Positions of two lakes in southeastern China; (b) water levels of Dongting Lake and (c) water levels of Poyang Lake (Yi et al., 2016).

4. Geographical Environment of South China

The terrain in Southern China is complex and includes mountains, hills, and basins. Therefore, the proportion of cultivated land area is relatively small. Figure S3 shows the map of vegetation classes aggregated from the 2007 MCD12C1 product modified from Chen et al. [1] (other woody vegetation (OWV)). The blue box is our study region, indicating that there are only two kinds of vegetation in Southern China (woody vegetation and crops, and most of them belong to the southern collective forest region). According to the research of Chen et al. [1], the greening in our study region is mainly due to trees, which relates to several ambitious programs to conserve and expand forests in order to control soil erosion, air pollution,

and climate change. Parts of the forests are plantations with rapidly growing young trees that are less than 40 years old.

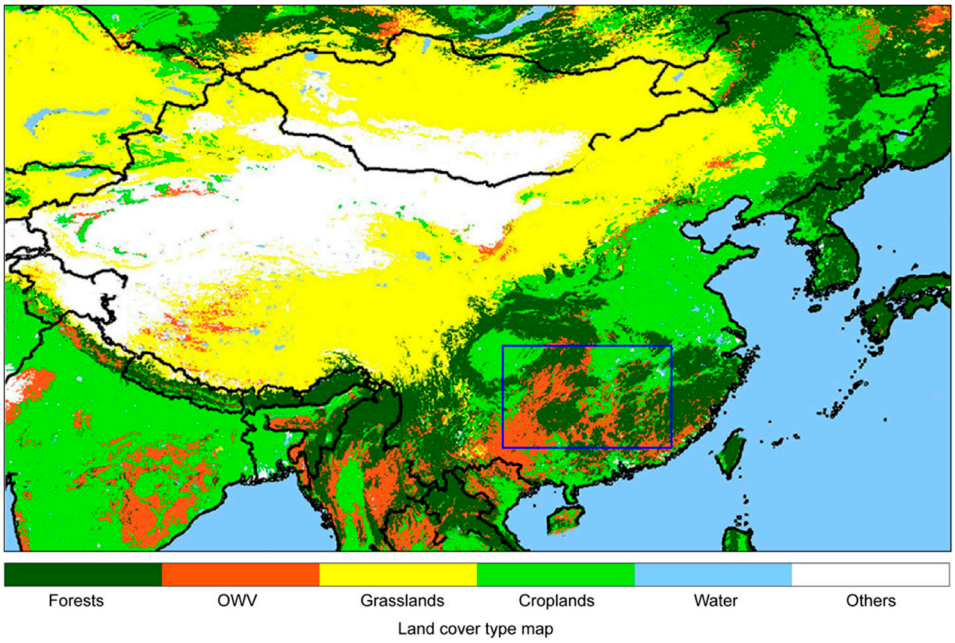

Figure S3. Map of vegetation classes aggregated from 2007 MCD12C1 product. OWV = other woody vegetation (after Chen et al., 2019).

5. Soil Water and Groundwater Change

5.1. Soil Water

The Global Land Data Assimilation System (GLDAS) dataset is calculated based on satellite and ground observational data using advanced land surface modeling and data assimilation techniques [3]. GLDAS drives four land surface models (LSMs): Mosaic, Noah, the Community Land Model (CLM), and the Variable Infiltration Capacity (VIC). We used the monthly L4 version 001 products with a spatial resolution of 1.0˚, provided by NASA Goddard Earth Sciences Data and Information Services Center (GESDISC, https://disc.gsfc.nasa.gov/datasets?keywords=GLDAS). The soil moisture and snow water equivalents data in these datasets were used as the total soil water.

Climate Prediction Center (CPC) soil moisture data [4] are model-calculated and are not measured directly. The data are monthly data with a spatial resolution of 0.5˚ (https://www.esrl.noaa.gov/psd/data/gridded/data.cpcsoil.html). CPC data do not contain snow water data, but there is little affect in our study region since it hardly snows.

We transformed each kind of monthly soil moisture data to spherical harmonic coefficients up to degree 60 from January 2003 to August 2016, and smoothed it with the DDK4 filter. We then calculated the mean soil water change within our study region, and the time series of five model (four GLDAS products and the CPC model) products are shown in Figure S4A. Figure S4B is the time series of five models after removing the seasonal change. It is obvious that the fluctuation of the Mosaic model is still too large relative to other models, and the fluctuation of CLM is too small to be real. Figure 4C, D (seasonal change removed) is the time series of Noah, VIC, and CPC, and they are consistent with each other. Therefore, we used these three products to calculate the soil water change.

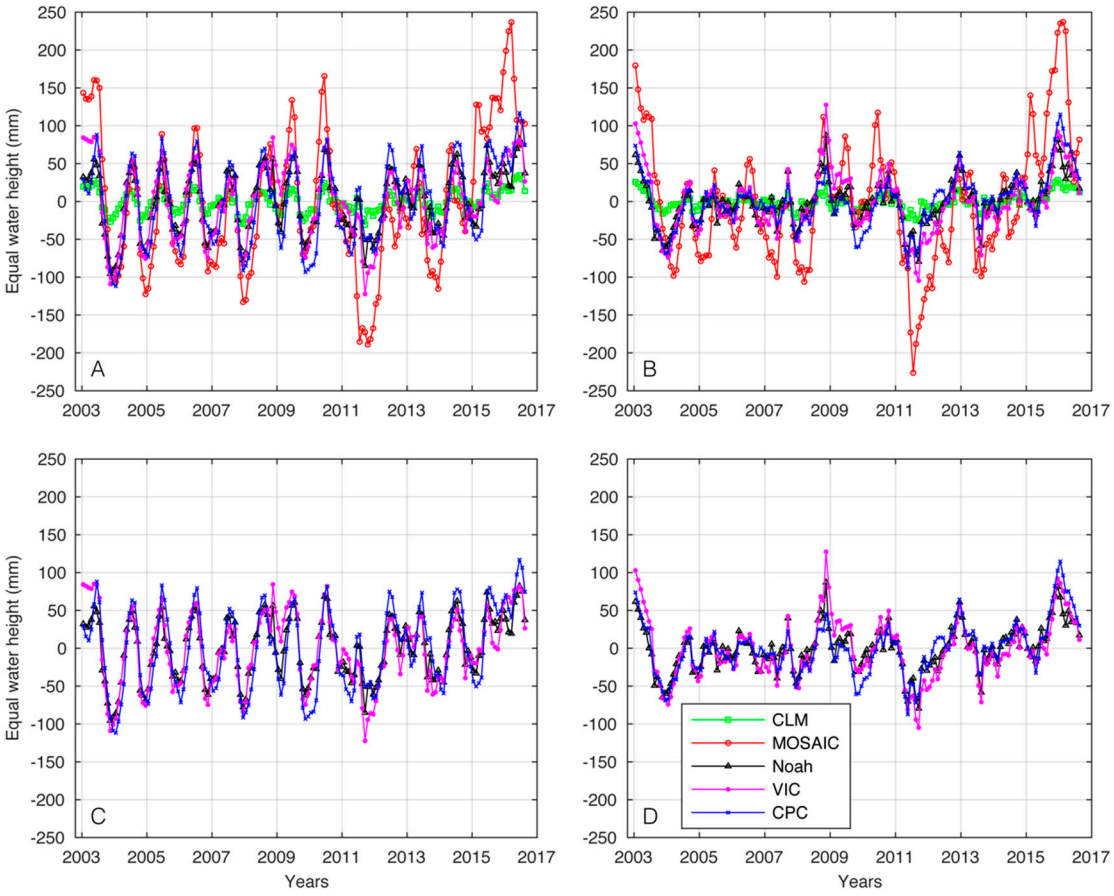

Figure S4. (A) time series of regional mean soil water change using four Global Land Data Assimilation System (GLDAS) products and a Climate Prediction Center (CPC) model from January 2003 to August 2018; (B) the seasonal change are removed; (C) Community Land Model (CLM) and MOSAIC data are removed from A and (D) seasonal changes are removed from C.

5.2. Groundwater

Seven global-scale groundwater stress indicators at the 0.5° grid-cell level and for trans-boundary aquifers larger than 20,000 km² were provided by Goethe University, Frankfurt (Germany). All the indicators were calculated based on the WaterGAP (Water–Global Assessment and Prognosis) model using daily values of temperature, precipitation, and long-wave and shortwave radiation for the period 1981–2010 from a homogenized version of the concatenated WATCH Forcing Data ERA-40 (WFD) and WFD ERA-Interim data sets (WFDEI). Herbert and Döll [5] provided a detailed description of the indicators. We used the indicator of "Monthly groundwater storage 2001–2010 from a model run with human water use". We transformed each month's groundwater data to spherical harmonic coefficients up to degree 60 and smoothed them with the DDK4 filter. Then, we calculated the region's mean groundwater change from 2003 to 2010, as shown in Figure S5. The red line is the time series after removing seasonality. The linear fitting shows that the ground water trend (0.6 mm/yr) is small relative to the greening trend (3.8 mm/yr).

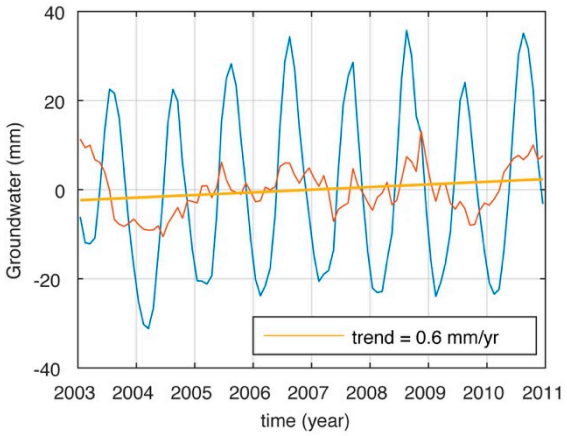

Figure S5. Time series of regional mean groundwater change from 2003 to 2010. The red line is the groundwater change after removing seasonality.

Reference

1. Chen, C.; Park, T.; Wang, X.; Piao,S.; Xu, B.; Chaturvedi, R.K.; Fuchs, R.; Brovkin, V.; Ciais, P.; Fensholt, R.; Tømmervik, H.; Bala, G.; Zhu,Z.; Nemani, R.R. and Myneni, R.B. China and India lead in greening of the world through land-use management. *Nat. Sustain.* **2019**, *2,* 122–129.
2. Yi, S.; Wang, Q.; Sun W. Basin mass dynamic changes in China from GRACE based on a multibasin inversion method. *J Geophys. Res.: Solid Earth* **2016**, *121*, 3782–3803.
3. Rodell, M.; Houser, P.R.; Jambor, U.; Gottschalck, J.; Mitchell, K.; Meng,C.-J.; Arsenault, K.; Cosgrove, B.; Radakovich, J.; Bosilovich, M.; et al. and Toll, D. The global land data assimilation system. *Bull. Am. Meteorol. Soc.* **2004**, *85*, 381–394.
4. Van den Dool, H.; Huang, J.and Fan, Y. Performance and analysis of the constructed analogue method applied to US soil moisture over 1981–2001. *J. Geophys. Res.: Atmos.* **2003**, *108, D16.*
5. Herbert, C. and Döll, P. Global assessment of current and future groundwater stress with a focus on transboundary aquifers. *Water Resour. Res.* 2019, 55, 4760–4784.